**Simulation of nanosizing effects in the decomposition of Ca(BH4)2 through atomistic thin film models**

Research on Chemical Intermediates

# Simulation of Nanosizing Effects in the Decomposition of Ca(BH4)2 through Atomistic Thin Film Models

--Manuscript Draft--

| | |
|---|---|
| **Manuscript Number:** | RINT-D-20-01231 |
| **Full Title:** | Simulation of Nanosizing Effects in the Decomposition of Ca(BH4)2 through Atomistic Thin Film Models |
| **Article Type:** | Original Research |
| **Keywords:** | Hydrogen storage materials, Calcium Borohydride, Nanostructuration, Decomposition Enthalpy, Quantum Mechanical Calculations |
| **Corresponding Author:** | Bartolomeo Civalleri, PhD<br>Department of Chemistry, University of Turin<br>Turin, Piemonte ITALY |
| **Corresponding Author Secondary Information:** | |
| **Corresponding Author's Institution:** | Department of Chemistry, University of Turin |
| **Corresponding Author's Secondary Institution:** | |
| **First Author:** | Elisa Albanese |
| **First Author Secondary Information:** | |
| **Order of Authors:** | Elisa Albanese |
| | Marta Corno |
| | Marcello Baricco |
| | Bartolomeo Civalleri, PhD |
| **Order of Authors Secondary Information:** | |
| **Funding Information:** | |
| **Abstract:** | In this work we model thin films of β-Ca(BH4)2 to understand how nanostructuration of the material can be an effective way to decrease the dehydrogenation enthalpy. Two different crystallographic faces of Ca(BH4)2 have been investigated (i.e. (001) and (101)) and two reaction pathways have been considered that release hydrogen through the formation of CaH2 and CaB6 , respectively. Quantum mechanical calculations predict that size reduction from bulk to nanoscale leads to a sizeable decrease of the decomposition enthalpy of the borohydride of about 5 kJ/mol H2 . Therefore, present results corroborate the evidence that nanostructured metal borohydrides show advantages for energy storage applications compared to their bulk counterparts. |

# Simulation of Nanosizing Effects in the Decomposition of $Ca(BH_4)_2$ through Atomistic Thin Film Models

E. Albanese,[1] M. Corno,[1] M. Baricco,[1] and B. Civalleri*[1]

[1]*Department of Chemistry, NIS and INSTM Reference Centre, University of Turin, Via Giuria 7, I-10125 Turin, Italy*

In this work we model thin films of $\beta$-$Ca(BH_4)_2$ to understand how nanostructuration of the material can be an effective way to decrease the dehydrogenation enthalpy. Two different crystallographic faces of $Ca(BH_4)_2$ have been investigated (i.e. (001) and (101)) and two reaction pathways have been considered that release hydrogen through the formation of $CaH_2$ and $CaB_6$, respectively. Quantum mechanical calculations predict that size reduction from bulk to nanoscale leads to a sizeable decrease of the decomposition enthalpy of the borohydride of about 5 kJ/mol$_{H_2}$. Therefore, present results corroborate the evidence that nanostructured metal borohydrides show advantages for energy storage applications compared to their bulk counterparts.

## I. INTRODUCTION

Metal borohydrides (MBHs) are very promising candidates as solid state hydrogen storage material because of their high gravimetric hydrogen content.[1–3] In particular, light-metal borohydrides possess a hydrogen wt% up to 17%. $Ca(BH_4)_2$ is, together with other alkali- and alkali-earth metal borohydrides (e.g. $Li(BH_4)$ and $Mg(BH_4)_2$), one of the most widely studied borohydride because of its high gravimetric capacity of hydrogen ($\approx$ 11.6 wt%).[4–8] However, the main drawbacks for technical applications of this class of compounds is the high hydrogenation/dehydrogenation temperature due to both thermodynamic and kinetic reasons. From a thermodynamic viewpoint, for a decomposition reaction of a generic solid hydrides if a $\Delta$S of 130 J/mol$_{H_2}$ is considered, which corresponds to the entropy change due to the formation of a gas ($H_2$) from a solid, it turns out that an equilibrium at room conditions (i.e. T = 300 K and $P_{eq}$ = 1 bar) is obtained for a $\Delta$H of about 30-40 kJ/mol$_{H_2}$.[9] Therefore, it is of considerable interest to find possible ways to destabilize the BHs and decrease the activation decomposition barrier, thus facilitating the release of molecular hydrogen.[9–11] In the search for the most promising ones, several strategies have been persued such as nanosizing, nanoconfinement and the inclusion of transition metals as additives.[12–16] In this work, we investigated from an atomistic point of view the effect of nanostructuring on the properties of the $Ca(BH_4)_2$[17–21] It is known by experimental evidence, that small size particles usually show different physical and chemical properties from the corresponding bulk materials.[16] They, indeed, show lower decomposition enthalpy with respect to the bulk.[22–25] In addition, the nanometric size of the particles allows for an easier diffusion of hydrogen through the material thus enhancing adsorption and desorption processes. Decreasing the particle size not only increases the specific surface area, but also the concentration of step, kink, and corner atoms, which most likely dominate the association and dissociation of hydrogen.[26] The thermodynamic properties of borohydrides can then be modified reducing significantly the particle size. In fact, the presence of free surfaces affect the free energy of both reagent and product phases, according to the Gibbs-Thompson effect.

It is clear that borohydride surfaces play a crucial role in the decomposition reaction process. Nevertheless, to our knowledge, a little is known about the surfaces of these materials and a few experimental work is available[27]. For this reason, we believe that a detailed study of the surface structure and of the size-decomposition enthalpy relationship is of primary importance to shed light on the decomposition process. Therefore, herein, we performed an accurate analysis on the $Ca(BH_4)_2$ surfaces by modeling crystallographic faces with different Miller indexes and evaluating their relative stability in order to predict the most stable one. Likely, this corresponds to the most exposed surface in the real system and in turn the one directly involved in the decomposition. To this purpose, the $Ca(BH_4)_2$ $\beta$-phase was selected because it is the most stable phase at high temperature and then it is directly involved in the decomposition reaction.[28] To simulate the surfaces, the so-called slab model approach was adopted.[29] The slab model consists of a film formed by the repetition of atomic layers parallel to a given (hkl) crystalline plane which identifies the surface. For sufficiently thick films, the slab model is expected to provide a faithful description of the real surface.[29] Finally, to evaluate the effect of nanosizing effects on the decomposition enthalpy of $\beta$-$Ca(BH_4)_2$, we took advantage of the slab model again by considering slabs of decreasing thickness. Even if this is not as modelling nano-particles it is an effective way to elucidate the role of the size of the system from bulk to very thin films. We have then considered two different decomposition reactions.

$$Ca(BH_4)_2 \rightarrow CaH_2 + 2B + 3H_2 \quad (1)$$

$$Ca(BH_4)_2 \rightarrow \frac{2}{3}CaH_2 + \frac{1}{3}CaB_6 + \frac{10}{3}H_2 \quad (2)$$

The first one leads to the undesired formation of boron, whereas the second pathway produces the most favorable $CaB_6$. Although Eq 1 is the most common decomposition

reaction, it has been reported in several works[7,8] that the production of $CaB_6$ and the absence of boron derivatives in Eq. 2 seems to permit the reversibility of the reaction at moderate condition[7].

This paper is organized as follow. In the next Section the theoretical methodologies are briefly discussed while in Section III the most relevant results are reported. First, the structure and stability of selected $Ca(BH_4)_2$ surfaces through thin film models is presented and then nanosizing effects on the decomposition enthalpy of the borohybride are discussed. Finally, the main conclusions are summarized in Section IV.

## II. COMPUTATIONAL DETAILS

The theoretical investigation of $Ca(BH_4)_2$ was carried out with periodic density functional theory (DFT) calculations employing the PBE functionals[30] as implemented in the CRYSTAL program[31]. An all electron 6-311G(d,p) basis set were used for all the atoms.

For the numerical integration of exchange-correlation term of all calculations, 75 radial points and 974 angular points (XLGRID) in a Lebedev scheme in the region of chemical interest were adopted. The Pack-Monkhorst/Gilat shrinking factors for the reciprocal space were set to 8. The accuracy of the integral calculations was increased by setting the tolerances to $10^{-8}$, $10^{-8}$, $10^{-7}$, $10^{-7}$, $10^{-18}$ a.u.. The self-consistent field (SCF) iterative procedure was converged to a tolerance in total energy of $\Delta E = 1 \cdot 10^{-7}$ a.u.. To accelerate convergence in the self-consistent calculations of the slab models a modified Broyden's scheme[32] following the method proposed by Johnson[33] was adopted. The above computational parameters ensured a full numerical convergence on all the computed properties described in this work. As regards the geometry optimization of the slab models, the atomic positions were optimized without any symmetry constraint and the cell parameters of the 2D unit cell were kept fixed at the bulk values. Vibrational frequencies at the $\Gamma$ point were calculated on the optimized geometry by means of a mass-weighted Hessian matrix, which is obtained by numerical differentiation of the analytical first derivatives.

In order to compute the enthalpy of decomposition (see eq. (1) and eq. (2)) at $T = 298.15$ K and $P = 1$ atm, the computed electronic energy $E_{el}$ was corrected for the zero point energy ($E_{ZPE}$), the thermal correction to enthalpy ($E_T(T)$) and the $P{\cdot}V$ (pressure $\cdot$ volume) contribution. The latter is negligible for solids and slabs at room pressure, while it corresponds to RT for molecules when considered to behave as an ideal gas. The enthalpy is then obtained as:

$$H(T) = E_{el} + E_{ZPE} + E_T(T) + RT \qquad (3)$$

These thermodynamic functions were obtained by summing the contribution of the vibrational modes at various points in the first Brillouin zone. Supercells with appropriate size were built in order to include phonon dispersion.

## III. RESULTS AND DISCUSSION

The $\beta$-phase belongs to the $P$-4 tetragonal space group and the unit cell contains two $Ca(BH_4)_2$ units. The computed cell parameters are $a = 6.65$ Å and $b = 4.39$ Å, in reasonably good agreement with the experimental data (the percentage deviation is -4.3% and 0.58%[34], respectively).

### A. Model surfaces

In the present work, we have considered the following low-index crystallographic faces: (100)=(010); (001); (101) and (111). Figure 1 shows the $\beta$-$Ca(BH_4)_2$ crystallographic unit cell and the side views of the unit cell perpendicular to the low-index crystallographic faces examined in the present work.

To simulate these surfaces within the slab model approach one has to start from the fully relaxed crystalline structure. Then, the following steps must be undertaken[29]: (i) select a given crystallographic face by specifying the corresponding (hkl) Miller indices; (ii) identify a suitable repeat unit (RU) which is usually made up of a few atomic layers; (iii) extract a thin film, formed by a finite number of repeat units, parallel to the crystallographic face. For the repeat unit to be acceptable, two basic requirements must be satisfied. Firstly, the stoichiometry must be preserved (or equivalently the model must be electroneutral, $q = 0$) and, secondly, the net dipole moment in the non-periodic direction (i.e. usually the $z$-axis) must be equal to zero ($\mu_z = 0$).

Among the four faces we have examined, only the (001) and the (101) model surfaces possessed a neutral repeat unit with $\mu_z = 0$. The two RUs are highlighted within red lines in Figure (1)). More details on the structural features of the two model surfaces will be given later on.

### B. Surfaces Stability and Structure

To identify the most stable face, the surface formation energy for the selected faces was evaluated by means of the following equation:

$$E_s = \lim_{n\to\infty} E_e(n) = \lim_{n\to\infty} \frac{E_n - n * E_{bulk}}{2A} \qquad (4)$$

where $E_n$ represents the energy of the optimized $n$-layers slab; $E_{bulk}$ is the energy of the repeat unit as in the bulk; $n$ is the number of RU in the slab model and $A$ is the area of the primitive 2D unit cell (fixed in the case of internal relaxation); $E_e(n)$ is the energy per unit area required to form an $n$-layers slab. $E_s$ is then the energy per unit area

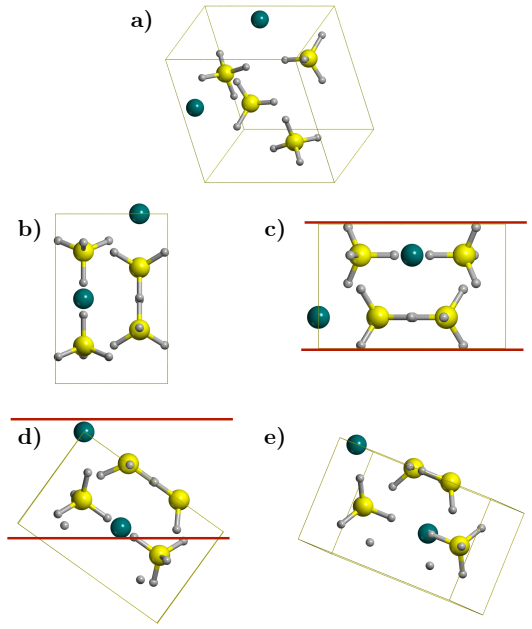


FIG. 1: $\beta$-$Ca(BH_4)_2$ crystallographic unit cell (a) and side views of the unit cell perpendicular to low-index crystallographic faces, namely: (100) (b), (001) (c), (101) (d) and (111) (e). The yellow spheres represent B atoms, white H atoms and green Ca atoms.

required to form the surface from the bulk crystal based on an $n$-layers slab model. As more layers are added in the calculation ($n \to \infty$), $E_e(n)$ will converge to the surface energy, i.e. $E_s$.

*a. (001) $Ca(BH_4)_2$ Surface.* In Figure 2a, the stoichiometric and non-polar repeat unit of the $Ca(BH_4)_2$ (001) surface, as cut out from the bulk, is displayed. It is comprised of five atomic layers (11 atoms) with a thickness of about 2.0 Å. Hereafter we denote it as 1-RU.

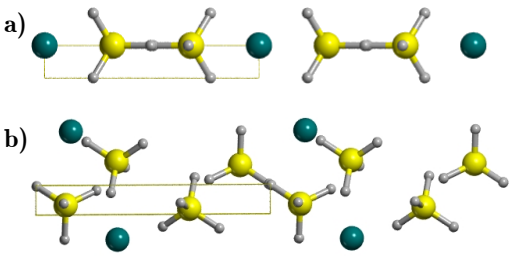


FIG. 2: Side view of non optimized 1-RU of (a) (001) and (b) (101) $Ca(BH_4)_2$ surfaces. The yellow spheres represent B atoms, white H atoms and green Ca atoms.

In order to compute the surface energy of formation, the thickness of the slab was increased up to 11-RU, which corresponds to a 2D unit cell of 143 atoms and a thickness of ≈22 Å. In particular, the surface formation energy was computed by using the Eq.4 for slab models from 1-RU up to 11-RU (see Figure 3).

In this case, the even numbers of repeat units were neglected; only odd number of RU has been considered. The reason is due to the fact that, in some cases, even and odd numbers of repeat units show different structural behavior.[35] Here, the packaging of the repeat units is shifted and $Ca^{2+}$ atoms lie on a zig-zag chain (Figure 3.1). To reproduce the same structural packing, it was therefore necessary to model only odd number of layers.

Figure 4 shows the $E_s$ convergence as function of the thickness of the films. Each point corresponds to a (001) $Ca(BH_4)_2$ slab model of increasing thickness (red points, Figure 4). The values slightly decrease by increasing the thickness, until a fairly good convergence is reached for the film containing 9-RU with $E_s$ around 0.19 J/m$^2$. The surface energy of a thick slab calculated with this approach coincides with the athermal surface energy at 0 K and zero pressure.

In Figure 3, the optimized structures of the different films with increasing thickness are reported. A relevant rearrangement of the top most layer, due to the relaxation of the surface, is evident, especially for thin slab models. Increasing the film size this behavior appears to be less important. As expected, the structural deformation extends to the inner layers, but it gradually decreases. For slabs that have reached the convergency (i.e. 9-RU and 11-RU with thickness of about 21 Å and 23 Å, respectively), the inner layers well reproduce the bulk structure. The structural changes of angles and bond lengths with respect to the $Ca(BH_4)_2$ bulk are discussed in the next paragraph.

*b. (101) $Ca(BH_4)_2$ Surface.* The suitable repeat unit of the (101) face is obtained by cutting a thin film (≈ 3.7 Å) terminating with a layer of metal ions, as shown in Figure 2b. Here, the packaging allows to take into account both even and odd number of layers. The stability and therefore the convergency of the surface is attained with the slab model constituted by 4-RU (thickness of 17.6 Å , Figure 4). The surface formation energy for the (101) $Ca(BH_4)_2$ slab model increases by increasing the thickness of the models and converges on a value for $E_s$ of 0.34 J/m$^2$. Also in this case, a strong rearrangement of the top most layers has been observed.

*c. Comparison of surfaces: structural analysis.* In order to quantitatively estimate the structural changes, the percentage difference ($\Delta$%) of the most relevant bond lengths of the optimized surfaces with respect to the values of the bulk structure is computed (Figure 5). In particular, we considered the $Ca(BH_4)_2$ formula units lying at the top most layer of the stabilized slab models, i.e 9-RU for (001) and 5-RU for (101), as depicted in Figure

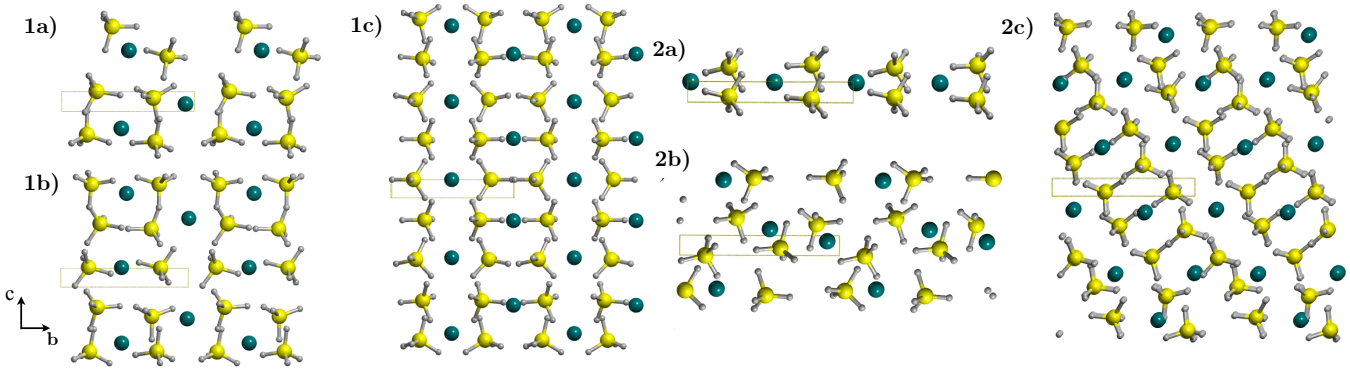


FIG. 3: Side view of three optimized slab models for each surfaces: 3-RU (1a), 4-RU (1b) and 9-RU (1c) for (001); 1-RU (2a), 2-RU (2b) and 5-RU (2b) for (101). The yellow spheres represent B atoms, white H atoms and green Ca. The yellow box in each structure represents the 2D periodic unit cell.

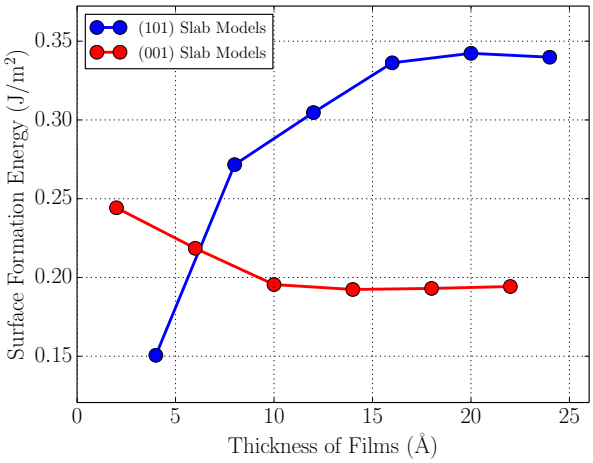


FIG. 4: Surface formation energy ($J/m^2$) of (001) (red curve) and (101) (blue curve) $Ca(BH_4)_2$ slab models as a function of slab thickness (in Å)

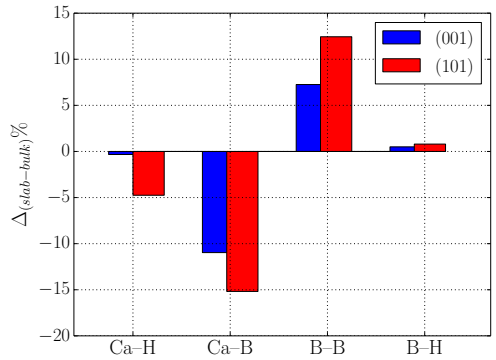


FIG. 5: Percentage differences of bond lenghts in the $Ca(BH_4)_2$ (001) and (101) slab model computed with respect to bulk structure (average values in Å: Ca-H=2.406; Ca-B=2.899; B-B=3.787 and B-H=1.230).

6. The bond lengths undergo huge changes: Ca–H and Ca–B decrease of about 10% in both cases, while B–B decrease of 15.6% in the (001) slab model and increase of 8.7% in the (101) (Figure 5). On the contrary, the B–H bond does not appear to be affected by the general transformation of the top most layer. Indeed, the $\Delta$% are less than 0.5% for both surfaces. As shown in Figures 6, the $BH_4^-$ ion changes its distance with respect the $Ca^{2+}$ cation and rotates up to find a new stable position at the surface.

Therefore, the (001) surface results as the most stable one. Its $E_s$ is indeed lower than that of the (101) $Ca(BH_4)_2$ slab model.

### C. Nanosizing Effects

By exploiting the slab models as obtained in section III B for both $Ca(BH_4)_2$ surfaces, we calculated the decomposition enthalpy as a function of the film thickness to mimick nanosizing effects.

The decomposition enthalpies of the $Ca(BH_4)_2$ thin films as function of the thickness of the film are reported in Figure 7 in comparison with the $\Delta$H value of the $Ca(BH_4)_2$ bulk, shown as a red line. As regards the Eq. 1, this value is around 52 $kJ/mol_{H_2}$, in good agreement with previous works[5,36]. Also, for the second decomposition reaction (see Eq. 2), the value obtained for the bulk structure, i.e. 34 $kJ/mol_{H_2}$, consistently agrees with known experimental and theoretical data.[5,36–38]

As shown in Figure 7, an overall decrease in the computed decomposition enthalpies is observed for films of reduced thickness. Not unexpectedly, the less stable face

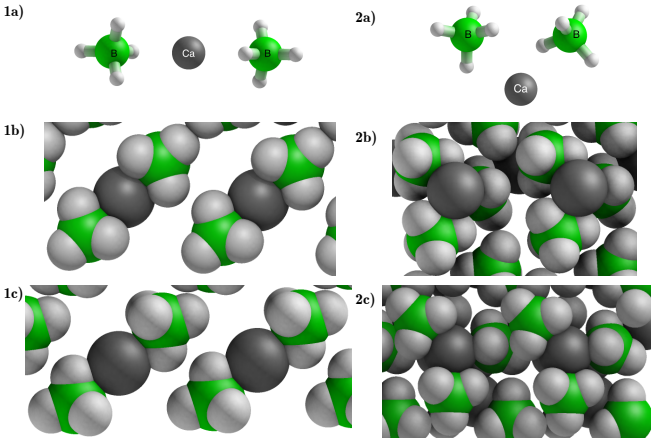


FIG. 6: Clusters cut from the (001) (1a) and (101) (2a) surfaces of the bulk. Top view of the top most layer of the 7-RU $Ca(BH_4)_2$ (001) and of the 4-RU $Ca(BH_4)_2$ (101) film before optimization (1b and 2b) and after optimization (1c and 2c). The dark grey, green and white spheres represent Ca, B and H, respectively.

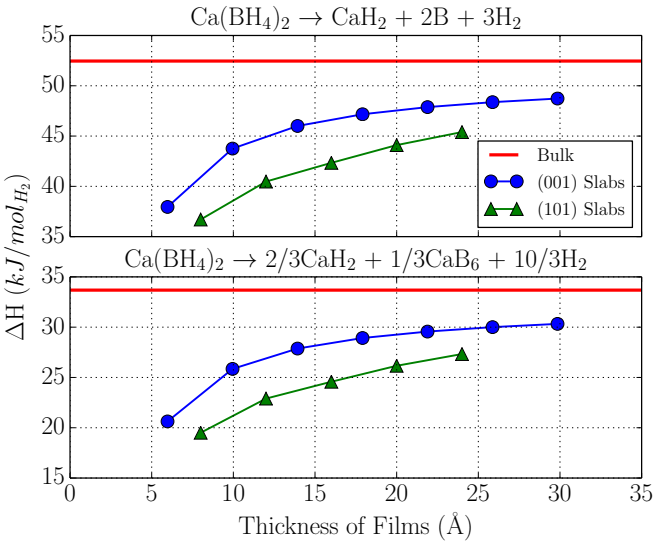


FIG. 7: Decompostion enthalpy ($kJ/mol_{H_2}$) as function of the film thickness (Å) of the $Ca(BH_4)_2$ (001) and (101) slab models for both Eq.1 and 2 (see text for details). The red line represents the $\Delta H$ of the $Ca(BH_4)_2$ bulk.

(i.e. (101)) shows a lower $\Delta H$. As discussed in the previous section, the borohydride groups of the (101) face are more exposed at the surface and then more prone to react.

For Eq. 1, the value of 30-35 $kJ/mol_{H_2}$, i.e. the target value for technical applications, is only reached for $Ca(BH_4)_2$ films with a very small thickness around 5 Å. Concerning the Eq. 2, the comparison between the two different decomposition pathways is quite important in light of the recent work by Sahle et al.[7]. Authors suggest, indeed, that the temperature of the reaction can promote the formation of $CaB_6$, thus making the reaction reversible. Our calculations confirm that according to the lower decomposition enthalpy of Eq. 2 the formation of $CaB_6$ is favored at low temperatures. It is worthy to note that for the (101) face the Ca-B and B-B shorter distances than in the bulk suggests that the formation of a Ca-B bond is likely more favoured than of a Ca-H bond, thus leading to $CaB_6$ rather than $CaH_2$. In addition, the target value of 30 $kJ/mol_{H_2}$ is reached for a slab thickness of 3 nm which is more realistic although still quite far from the actual size of a nanoparticle.

Interestingly, for both reactions, the convergence toward the bulk limit is very slow. In fact, even for the thickest slab model (i.e. 28 Å) $\Delta H$ does not significantly approach the red line as shown in Figure 7. It turns out that even if the thickness required to obtain a value around 30-35 $kJ/mol_{H_2}$ is very small from an experimental point of view (usually around 10 nm), the comparison with respect to the bulk value shows that, at nanoscale, a bulk-to-surface transition allows one to gain at least 5 $kJ/mol_{H_2}$ in the decomposition enthalpy.

Overall, present results clearly show that the formation of small particles of borohydride leads to a net decrease of the $\Delta H$ with respect to the bulk thus confirming that nanostructuraction is a valuable approach to favor the release of hydrogen.

## IV. SUMMARY AND CONCLUSIONS

The nanosizing effect on the $Ca(BH_4)_2$ decomposition reaction has been evaluated by modelling thin films of different thickness by means of quantum-mechanical calculations. In particular, the $\beta$-$Ca(BH_4)_2$ polymorph was selected because it is the most stable one at high temperature and then it is directly involved in the decomposition reaction.

Different low-index crystallographic faces of the $\beta$-$Ca(BH_4)_2$ crystal and their relative stability were investigated. We have shown that only two faces are physically stable, namely: (001) and (101), while the (100) and (111) faces do not satisfy the electroneutrality and non-polarity conditions. Therefore, it is expected (001) and (101) faces could be exposed at the surface in real crystallite in powder samples. The most stable surface is the (001) with a surface formation energy of 0.19 $J/m^2$ while the (101) face shows a slightly higher $E_s$ of 0.34 $J/m^2$.

We have also evaluated the nanosizing effects by considering the variation of the decomposition enthalpy $\Delta H$ as a function of the film thickness for two different decomposition pathways leading to $CaH_2$ and $CaB_6$, respectively.

The results show that the $\Delta H$ values decrease for films of decreasing thickness until to reach the target value of 30-35 $kJ/mol_{H_2}$ for thin films of ranging from 5 to 20 Å. Not unexpectedly, the lower the stability of the surface

the lower the decomposition enthalpy. Therefore, computed results show that nanostructured $Ca(BH_4)_2$ can be a good candidate for solid state hydrogen storage.

Overall, our work confirms that nanostructuring of metal borohydrides is an effective way to generates nanoparticles with different faces exposed at the surface that, according to their stability, show a lower decomposition enthalpy. Analogously, it is expected that nanoconfiment through permeation into scaffolds would lead to a similar decrease of $\Delta H$.[39–41] Size reduction from bulk to nanoscale is then a valuable method to tune the thermodynamics of hydrogen release from metal borohydrides[24,25].


[1] S. Orimo, Y. Nakamori, J. Eliseo, A. Züttel, and C.M. Jensen. Complex hydrides for hydrogen storage. *Chem. Rev.*, 107:4111–4132, 2007.

[2] L. Schlapbach and A. Züttel. Hydrogen-storage materials for mobile applications. *Nature*, 414:353–358, 2001.

[3] Y. Nakamori and S. Orimo. *Borohydrides as hydrogen storage materials. In Solid-State Hydrogen Storage.* Woodhead Publishing Limited: Cambridge, UK, 2008.

[4] Ewa Rönnebro and Eric H. Majzoub. Calcium borohydride for hydrogen storage: catalysis and reversibility. *The Journal of Physical Chemistry B*, 111(42):12045–12047, 2007. PMID: 17914804.

[5] J. Mao, Z. Guo, C. K. Poh, A. Rajbar, Y. Guo, X. Yu, and H. Liu. *J. Alloys and Compd.*, 500:200–205, 2010.

[6] Isabel Llamas-Jansa, Oliver Friedrichs, Maximilian Fichtner, Elisa Gil Bardaji, Andreas Züttel, and Bjørn C. Hauback. The role of ca(bh4)2 polymorphs. *The Journal of Physical Chemistry C*, 116(25):13472–13479, 2012.

[7] C. J. Sahle, C. Sternemann, C. Giacobbe, Y. Yan, C. Weis, M. Harder, Y. Forov, G. Spiekermann, M. Tolan, M. Krischa, and A. Remhof. Formation of cab6 in the thermal decomposition of the hydrogen storage material ca(bh4)2. *Phys. Chem. Chem. Phys.*, 18:19866, 2016.

[8] Y. Yan, A. Remhof, D. Rentsch, A. Züttel, S. Girief, and P. Jenae. A novel strategy for reversible hydrogen storage in ca(bh4)2. *Chem. Commun.*, 51:11008, 2015.

[9] M. Baricco, M. Palumbo, E. Pinatel, M. Corno, and P. Ugliengo. Thermodynamic database for hydrogen storage materials. *Adv. Science Technol.*, 72, 2010.

[10] Y. Filinchuk, D. Chernyshov, and V Dmitriev. *Z. Kristallogr.*, 223:649– 659, 2008.

[11] V.A. Yartys, M.V. Lototskyy, E. Akiba, R. Albert, V.E. Antonov, J.-R. Ares, M. Baricco, N. Bourgeois, C.E. Buckley, J.M. Bellosta von Colbe, J.-C. Crivello, F. Cuevas, R.V.Denys, M.Dornheim, M.Felderhoff, D.M. Grant, B.C. Hauback, T.D. Humphries, I. Jacob, T.R. Jensen, P.E.deJongh, J.-M.Joubert, M.A. Kuzovnikov, M. Latroche, A. Montone, M. Paskevicius, L. Pasquini, L. Popilevsky, V.M. Skripnyuk, E. Rabkin, V. Sofianos, A. Stuart, G. Walker, H. Wang, C.J. Webb, and M. Zhu. Magnesium based materials for hydrogen based energy storage: past, present and future. *Int. J. Hydrog. Energy*, 44:78097859, 2019.

[12] A. J. Du and S. C. Smith. *Phys. Rev. B: Condens. Matter*, 74:193405, 2006.

[13] A. Ampoumogli, Th. Steriotis, P. Trikalitis, E. Gil Bardaji, M. Fichtner, A. Stubos, and G. Charalambopoulou. *International Journal of Hydrogen Energy*, 37:16631–16635, 2012.

[14] B. Zhai, X. Xiao, W. Lin, X. Huang, X. Fan, S. Li, H. Ge, Q. Wang, and L. Chen. Enhanced hydrogen desorption properties of libh4eca(bh4)2 by a synergetic effect of nanoconfinement and catalysis. *Int. J. Hydrogen Energy*, 41:17462–17470, 2016.

[15] G. Xia, Y. Tan, F. Wu, F. Fang, D. Sun, Z. Guo, Z. Huang, and X. Yu. Graphene-wrapped reversible reaction for advanced hydrogen storage. *Nano Energy*, 26:488–495, 2016.

[16] A. Schneemann, J.L. White, S.Y. Kang, S. Jeong, L.F. Wang, E.S. Cho, T.W. Heo, D. Prendergast, J.J. Urban, B.C. Wood, M.D. Allendorf, and V. Stavila. Nanostructured metal hydrides for hydrogen storage. *Chem. Rev.*, 118:1077510839, 2018.

[17] H. Majzoub and E. Rönnebro. Crystal structures of calcium borohydride: Theory and experiment. *J. Phys. Chem. C*, 113:3352–3358, 2009.

[18] T. J. Frankcombe. Calcium borohydride for hydrogen storage: A computational study of $ca(bh_4)_2$ crystal structures and the $cab_2h_x$ intermediate. *J. Phys. Chem. C*, 114:9503–9509, 2010.

[19] H. Grove, L.H. Rude, T.R. Jensen, M. Corno, P. Ugliengo, M. Baricco, M.H. Srby, and B.C. Hauback. Halide substitution in ca(bh4)2. *RSC Adv.*, 4:4736–4742, 2014.

[20] M. Gr T.A. Boynuegri. Catalytic dehydrogenation of calcium borohydride by using hydrogel catalyst. *Int. J. Hydrog. Energy*, 42:17869–17873, 2017.

[21] E. M. Dematteis, S. R. Jensen, T. R. Jensen, and M. Baricco. Heat capacity and thermodynamic properties of alkali and alkali-earth borohydrides. *J. Chem. Theormodynamics*, 143:106055, 2020.

[22] A. Pundt and R. Kirchheim. *Ann. Rev. Mater. Res.*, 36:555 – 608, 2006.

[23] M. Yamauchi, R. Ikeda, H. Kitigawa, and M. Takata. *J. Phys. Chem. C*, 112:3294 – 3299, 2008.

[24] T. K. Nielsen, F. Besenbacher, and T. R. Jensen. Nanoconfined hydrides for energy storage. *Nanoscale*, 3:2086–2098, 2011.

[25] L. K. Wagner, E. H. Majzoub, M. D. Allendorf, and J. C. Grossman. Tuning metal hydride thermodynamics via size and composition: Lih, mgh, alh, and mgalh nanoclusters for hydrogen storage. *Phys. Chem. Chem. Phys.*, 14:6611–6616, 2012.

[26] P. E. de Jongh and P. Adelhelm. *ChemSusChem*, 3:1332–1348, 2010.

[27] R. Wu, Z. Ren, X. Zhang, Y. Lu, H. Li, M. Gao, H. Pan, and Y. Liu. Nanosheet-like lithium borohydride hydrate with 10 wt % hydrogen release at 70 c as a chemical hydrogen storage candidate. *J. Phys. Chem. Lett.*, 10:18721877, 2019.

[28] Y. Filinchuk, E. Rönnebro, and D. Chandra. *Acta Mater.*, 57:732–738, 2009.

[29] R Dovesi, B. Civalleri, R. Orlando, C. Roetti, and V. R. Saunders. Ab initio quantum simulation in solid state chemistry. *Rev. Comp. Chem.*, 21:1–125, 2005.

[30] J. P. Perdew, K. Burke, and M. Ernzerhof. *Phys. Rev.*

*Lett.*, 77:3865, 1996.

[31] R. Dovesi, V. R. Sauders, C. Roetti, R. Orlando, C. M. Zicovich-Wilson, F. Pascale, B. Civalleri, K. Doll, N. M. Harrison, I. J. Bush, P. D'Arco, and M. Llunell. *CRYSTAL09*, University of Torino, Torino, 2009.

[32] C. G. Broyden. *Math. Comput.*, 19:577–593, 1965.

[33] D. D. Johnson. *Phys. Rev. B*, 38:12807–12813, 1988.

[34] F. Buchter, Z. Łodziana, A. Remhof, O. Friedrichs, A. Borgschulte, Ph. Mauron, A. Züttel, D. Sheptyakov, G. Barkhordarian, R. Bormann, K. Chłopek, M. Fichtner, M. Sørby, M. Riktor, B. Hauback, and S. Orimo. *J. Phys. Chem. B*, 112:8042–8048, 2008.

[35] J. Scaranto, G. Mallia, S. Giorgianni, C.M. Zicovich-Wilson, B. Civalleri, and N.M. Harrison. *Surface Science*, 600:305–317, 2006.

[36] Y. Kim, D. Reed, Y.S. Lee, J.Y. Lee, J.H. Shim, D. Book, and Y.W. Cho. *J. Phys. Chem. C*, 113:5865–5871, 2009.

[37] K. Miwa, M. Aoka, T. Noritake, N. Ohba, Y. Nakamori, S. Towata, A. Züttel, and S. Orimo. *Phys. Rev. B: Condens. Matter Mater. Phys.*, 74:155122, 2006.

[38] V. Ozolins, E. H. Majzoub, and C. Wolverton. *J. Am. Chem. Soc.*, 131:230–237, 2009.

[39] P. E. de Jongh, M. Allendorf, J. J. Vajo, and C. Zlotea. Nanoconfined light metal hydrides for reversible hydrogen storage. *MRS Bulletin*, 38:488–494, 2013.

[40] Q. Lai, Y. Yang, Y. Sun, and K.F. AgueyZinsou. Nanoconfinement of borohydrides in hollow carbon spheres: Melt infiltration versus solvent impregnation for enhanced hydrogen storage. *Int. J. Hydrog. Energy*, 44:23225–23238, 2019.

[41] A. Schneemann, L.F. Wan, A.S. Lipton, Y.-S. Liu, J.L. Snider, A.A. Baker, J.D. Sugar, C.D. Spataru, J. Guo, T.S. Autrey, M. Jrgensen, T.R. Jensen, B.C. Wood, M.D. Allendorf, and V.Stavila. Nanoconfinement of molecular magnesium borohydride captured in a bipyridine-functionalized metalorganic framework. *ACS Nano*, 14:10294–10304, 2020.